

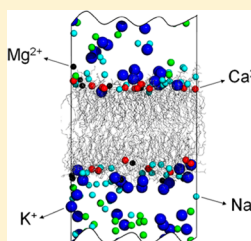
Binding Competition to the POPG Lipid Bilayer of Ca^{2+} , Mg^{2+} , Na^+ , and K^+ in Different Ion Mixtures and Biological Implication

Yanyan Mao, Yun Du, Xiaohui Cang, Jinan Wang, Zhuxi Chen, Huaiyu Yang,* and Hualiang Jiang*

Drug Discovery and Design Center, State Key Laboratory of Drug Research, Shanghai Institute of Materia Medica, Chinese Academy of Sciences, 555 Zuchongzhi Road, Shanghai 201203, China

Supporting Information

ABSTRACT: Ion mixtures are prevalent in both cytosol and the exterior of a plasma membrane with variable compositions and concentrations. Although abundant MD simulations have been performed to study the effects of single ion species on the structures of lipid bilayers, our understanding of the influence of the ion mixture on membranes is still limited; for example, the competition mechanism of different ions in binding with lipids is not clearly addressed yet. Here, microsecond MD simulations were carried out to study the effects of the mixtures of Ca^{2+} , Mg^{2+} , Na^+ , and K^+ ions on a 1-palmitoyl-2-oleoyl-*sn*-glycero-3-phosphoglycerol (POPG) bilayer. It has been revealed that the binding efficiency of these ions with POPG lipids is in the following order, $\text{Ca}^{2+} > \text{Mg}^{2+} > \text{Na}^+ > \text{K}^+$. The binding free energy of Ca^{2+} to the lipid bilayer is ~ -4.0 kcal/mol, which is much lower than those of other ions. This result explains why the effects of the ion mixture on membranes are particularly sensitive to the concentration of calcium. The on-rates of different ions do not have a large difference, while the off-rate of Ca^{2+} is 2–3 orders of magnitude smaller than those of the others. Therefore, the strongest binding affinity of Ca^{2+} is mainly determined by its smallest off-rate. In addition, our study suggests that the structure of the lipid bilayer is influenced dominantly by the concentration of Ca^{2+} ions. The simulation results also provide a good explanation for a variety of biological processes relevant to Ca^{2+} and Mg^{2+} regulations, such as membrane fusion.



	Ca^{2+}	Mg^{2+}	Na^+	K^+
ΔPMF (kcal/mol)	-4.2	-2.5	-1.5	-1.0
k'_{on} ($10^9 \text{ mol}^{-1} \text{ s}^{-1}$)	43	52	2.5	3.1
k_{off} (10^9 s^{-1})	0.0036	0.50	1.1	2.1

INTRODUCTION

Ions directly interact with membrane lipids and thus influence structural and functional properties of membranes,^{1–6} such as membrane packing and fusion, signal transduction across membranes, as well as membrane protein binding and their insertion.^{7–13} In a physiological environment, ions are prevalent in both cytosol and the exterior of the membrane with spatially and temporally variable compositions and concentrations. To understand the effects of the ion mixture on membranes, both the effects of single-ion species and the competition of different ions in binding with lipids should be elucidated.

Molecular dynamics (MD) simulation generates the images of the interaction between ions and membrane bilayers at the atomic level and has been widely used to study the effects of ions on lipid bilayers.^{14–18} Previous MD simulations have obtained numerous consistent results with experiments in elucidating the effects of ions on various properties of the lipid bilayers, such as the acyl chain order parameter,¹⁹ cation location in the bilayer surface, area per lipid, and phase transition.²⁰ Moreover, the MD simulation approach complements the experimental results to reveal the atomic characteristics for the ion–phospholipid binding stoichiometry and the detailed binding processes.¹⁴ However, as most of the simulations have paid attention to the effects of individual ion species on the lipid bilayers, the simultaneous binding of

several different ions to the lipids has not been fully appreciated yet. Additionally, calculating the thermodynamics and kinetics parameters of ion binding with lipids is still a challenge.

In order to get insights into some key issues related to the ion mixture effects on the membrane, we performed two MD simulations on ion–lipid bilayer systems consisting of an ion mixture of Ca^{2+} , Mg^{2+} , Na^+ , K^+ , and Cl^- ions and anionic 1-palmitoyl-2-oleoyl-*sn*-glycero-3-phosphoglycerol (POPG) lipids. On the basis of the simulation trajectories, we quantitatively measured the binding affinities of the four cations and their binding kinetics parameters to the lipids. The results suggested that the binding modes of Mg^{2+} , Na^+ , and K^+ to the lipids are influenced by the concentration of Ca^{2+} . The outstanding ability and special property of Ca^{2+} binding to anionic lipids makes it a universal and versatile role in membrane-involved life processes.

METHODS

Simulation Systems. Starting from a 2-oleoyl-1-palmitoyl-*sn*-glycero-3-phosphocholine (POPC) bilayer containing 128 lipid molecules generated by VMD,²¹ the POPG (Figure 1) bilayer was built by substituting the choline head group with

Received: October 15, 2012

Revised: December 25, 2012

Published: December 27, 2012

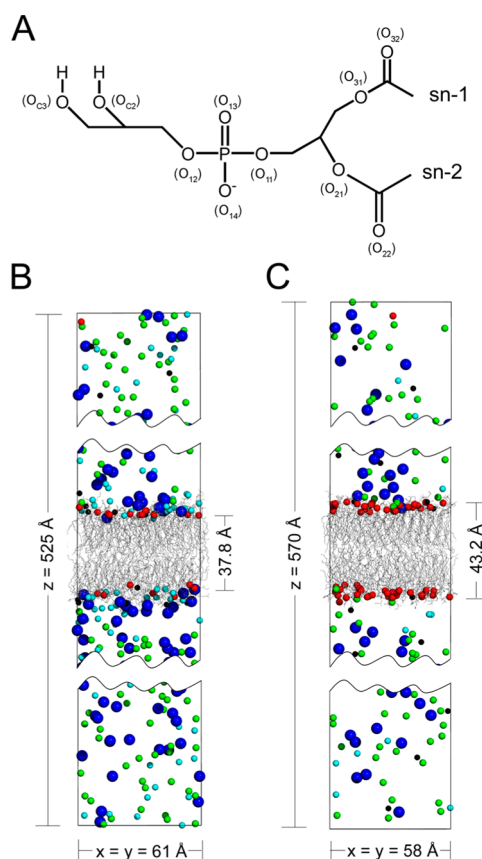


Figure 1. (A) Chemical structure of POPG. The names of the oxygens in the parentheses are following those in the CHARMM27 force field. (B,C) Side views of the last snapshots that resulted from simulation systems I (B) and II (C). Ca^{2+} , Mg^{2+} , Na^+ , K^+ , and Cl^- ions are shown as red, black, cyan, blue, and green balls, respectively. Phospholipids are displayed as light gray lines. Hydrogen atoms and water molecules are not presented for clarity. The lengths of the simulation boxes (x , y , and z axes) and the thicknesses of the hydrophobic parts of the lipid bilayers are labeled.

glycerol. Two systems of POPG lipid bilayers with ion mixtures of four cations (Ca^{2+} , Mg^{2+} , Na^+ , and K^+) that most abundantly exist in physiological conditions were constructed. Because the physiological concentrations of Na^+ and K^+ ions are much higher than those of Ca^{2+} and Mg^{2+} ions, we constructed the first POPG bilayer with 20 Ca^{2+} , 20 Mg^{2+} , 160 Na^+ , and 160 K^+ ions (system I). In order to consider the specific case that the temporal concentration of calcium ions may arise locally and meanwhile produce the different ion concentrations compared to the first bilayer, a second POPG bilayer with 60 Ca^{2+} , 40 Mg^{2+} , 40 Na^+ , and 80 K^+ ions (system II) was generated. Cl^- ions were added to both systems as counterions. Each system was solvated by ~ 58000 TIP3P²² water molecules.

MD Simulation. All of the simulations were carried out with the GROMACS4.5.3 package,²³ with the NPT ensemble and periodic boundary conditions. The CHARMM27 force field was applied.^{24–26} Energy minimization was performed to relieve unfavorable contacts inside of systems. Then, the temperature of the system was maintained at 300 K using the v-rescale method²⁷ with a coupling time of 0.1 ps. The pressure was kept at 1 atm by semi-isotropically coupling using the Berendsen method²⁸ with a coupling constant of 1.0 ps and a compressibility of $4.5 \times 10^{-5} \text{ bar}^{-1}$. The time step for integration was set to 0.002 ps. The hydrogen-involved

covalent bonds in water molecules and others were constrained using the SETTLE²⁹ and LINCS³⁰ algorithms, respectively. The electrostatic interactions were calculated using the Particle Mesh Ewald (PME) algorithm.³¹ A cutoff value of 1.2 nm was used for both electrostatic and van der Waals interactions calculations. Each system was independently run for 600 ns three times so as to enhance sampling. The total simulation time of the two systems reached 3.6 μs . The coordinates of the simulation systems were recorded every 10 ps. The last 100 ns of MD trajectories of each of the six runs were used for analysis.

Calculation of the Potential Mean Force (PMF). Instead of the absolute z -coordinate, the distance between each ion and its nearest phosphorus atom in the normal direction (z -axis) was calculated as the reaction coordinate ζ to avoid a possible flattening of PMF due to the fluctuation of the membrane thickness. An individual ion in each snapshot that was extracted from three 100 ns trajectories at 10 ps intervals for each system was taken as one sampling. For each system, 3×10^4 snapshots were isolated from the three MD trajectories (10^4 snapshots from each trajectory), and each snapshot contained 20 Ca^{2+} , 20 Mg^{2+} , 160 Na^+ , and 160 K^+ for system I and 60 Ca^{2+} , 40 Mg^{2+} , 40 Na^+ , and 80 K^+ for system II. Thus, the sampling numbers of Ca^{2+} , Mg^{2+} , Na^+ , and K^+ were 6×10^5 , 6×10^5 , 4.8×10^6 , and 4.8×10^6 for system I and 1.8×10^6 , 1.2×10^6 , 1.2×10^6 , and 2.4×10^6 for system II. The reaction coordinate was divided into 260 windows from -10 to 250 Å. For each ion species, the probability of its appearance in each window (P_ζ) was calculated. The average PMF for the ion in aqueous solution was set to 0, and the PMF of reaction coordinate ζ ($W(\zeta)$) was calculated by eq 1.³²

$$W(\zeta) = -k_B T \ln \frac{P_\zeta}{P_\zeta^*} \quad (1)$$

where k_B is the Boltzmann constant, T is the absolute temperature, P_ζ refers to the probability that the ion appeared in the window at reaction coordinate ζ , and P_ζ^* is the average probability that the ion appeared in a window in the solution.

Calculation of Kinetics Parameters. In order to investigate the kinetic properties of ion–lipid binding and unbinding, we mapped these processes onto a simple binary state of a ligand–receptor model.^{33,34} The ion-binding site (S) on the membrane was regarded as a receptor; every ion (I) was taken as a ligand, and each ion–lipid complex (IS) was viewed as a ligand–receptor complex.



In the present study, on the basis of the long time simulation trajectories, we calculated the on-rate (k_{on}) of ion binding and off-rate (k_{off}) of ion unbinding. Assuming that the unbinding process is a zero-order reaction, k_{off} is only dependent on the mean time for one unbinding event (t_{off})^{33,34}

$$k_{\text{off}} = \frac{1}{t_{\text{off}}} \quad (3)$$

t_{off} of each ion species could be calculated by eq 4

$$t_{\text{off}} = \frac{T_{\text{bound}}}{N_{\text{off}}} \quad (4)$$

where T_{bound} is the sum of the time of the ion staying in the lipid bilayer and N_{off} is the number of unbinding events of the ion during the simulations.

Table 1. Numbers of Total Ions, Bound Ions, Unbound Ions, Lipids Per Bound Ion, and Oxygens Per Bound Ion

	system I				system II			
	Ca ²⁺	Mg ²⁺	Na ⁺	K ⁺	Ca ²⁺	Mg ²⁺	Na ⁺	K ⁺
no. of total ions	20	20	160	160	60	40	40	80
no. of bound ions	18.7 ± 0.5	9.8 ± 1.5	34.1 ± 4.5	24.7 ± 3.9	55.5 ± 1.1	4.9 ± 1.6	3.5 ± 1.6	4.2 ± 1.5
no. of unbound ions	1.3 ± 0.5	10.2 ± 1.5	125.9 ± 4.5	135.3 ± 3.9	4.5 ± 1.1	35.1 ± 1.6	36.5 ± 1.6	75.8 ± 1.5
no. of lipids per ion	4.0 ± 0.5	2.4 ± 1.1	2.7 ± 1.1	2.7 ± 1.2	3.9 ± 0.8	2.0 ± 1.0	1.9 ± 1.1	2.4 ± 1.2
no. of oxygens per ion	5.7 ± 0.4	3.9 ± 0.8	6.6 ± 1.1	6.7 ± 1.3	5.3 ± 0.2	3.1 ± 1.2	4.7 ± 3.5	5.9 ± 4.0

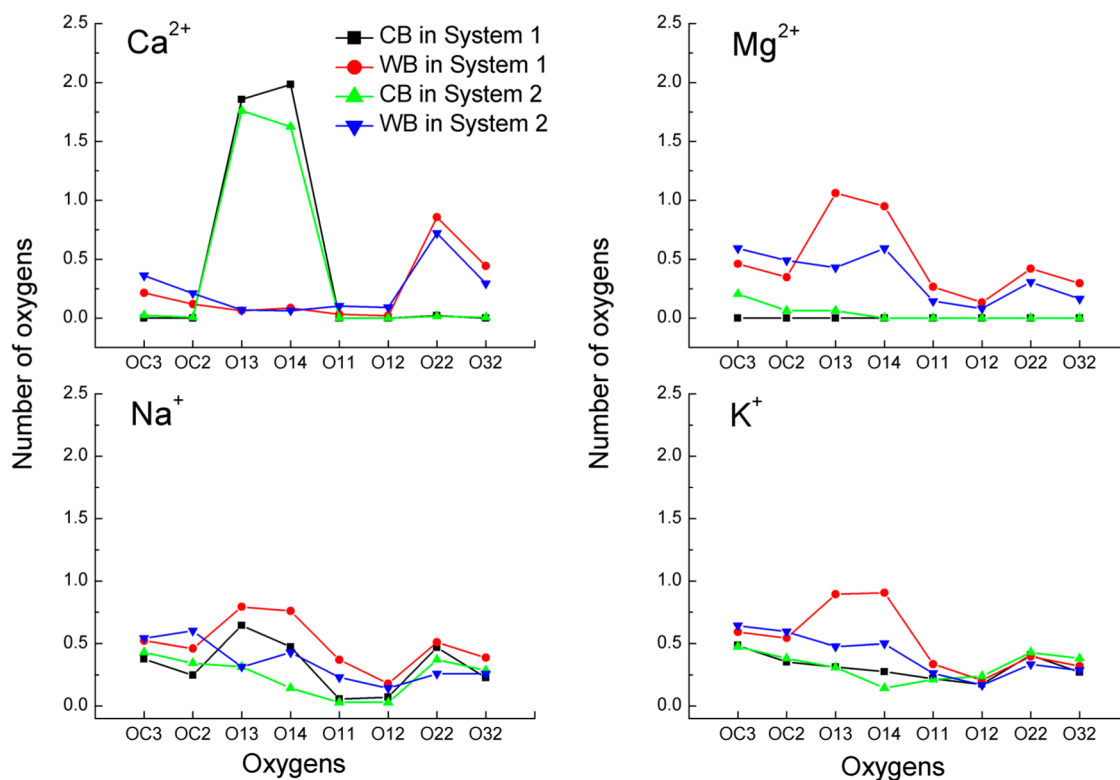


Figure 2. Average number of oxygens per ion involved in forming direct coordination bonds (CBs) or water bridges (WBs) with ions.

Assuming that the binding process is a first-order reaction, k_{on} is related to the mean time for a binding event on one binding site (t_{on}) and the concentration of the ion in bulk [I]

$$k_{\text{on}} = \frac{1}{t_{\text{on}}[I]} \quad (5)$$

In MD simulations, the available free binding sites for ions on the lipid bilayer are not only multiple but also variable due to the structural changes of the bilayer. Thus, it is difficult to measure the mean time for a binding event on one binding site. Instead, the mean time for a binding event on the whole lipid bilayer in simulation (t'_{on}) is measurable

$$t'_{\text{on}} = \frac{T_{\text{unbound}}}{N_{\text{on}}} \quad (6)$$

where T_{unbound} is the sum of the time of the ion staying in the bulk in simulation and N_{on} is the number of binding events. Therefore, we calculated a modified on-rate (k'_{on})

$$k'_{\text{on}} = \frac{1}{t'_{\text{on}}[I]} \quad (7)$$

where [I] is the ion concentration. k_{on} is the association constant of the ligand binding to one site, and the calculated

k'_{on} is the association constant of the ion binding on all of the free binding sites in the lipid bilayer. Accordingly, our calculated k'_{on} is higher than k_{on} . Nevertheless, for one lipid system, because the free ion-binding sites are almost the same for all ions, $k'_{\text{on}}/k_{\text{on}}$ is a constant for all ions. Therefore, the calculated k'_{on} values in the current study could semi-quantitatively reflect the “on abilities” of different ions.

RESULTS

Numbers of Bound Ions. Simulations revealed that each ion may interact with a lipid bilayer with two modes, directly coordinating with the lipid oxygens and indirectly interacting with the lipid through a water bridge, that is, the ion coordinates with a water molecule that further hydrogen bonds to a lipid oxygen (Figure S1, Supporting Information). We refer to ions interacting with lipids with either mode as bound ions. The effects of an ion mixture on the lipid bilayer structures are directly associated with the composition of the bound ions in the bilayer. Therefore, the bound ions in the two simulation systems were analyzed first. Figure S2 (Supporting Information) shows the time evolution of the numbers of bound Ca²⁺, Mg²⁺, Na⁺, and K⁺ ions in the two simulation systems. As mentioned above, the MD trajectory of each bilayer was repeated three times; only one of the three was taken as an

example shown in Figure S2 (Supporting Information). It was found that only after 200 ns did the numbers of the bound ions reach equilibrium, indicating that a long time is critical for the MD simulations to study the effect of the ion mixture on the lipid bilayer. After reaching the equilibrium, the fluctuation of the number of bound Ca^{2+} ions is the smallest one among the four profiles, while the numbers of bound Na^+ and K^+ ions have a larger fluctuation amplitude than those of Ca^{2+} and Mg^{2+} , in particular, in the simulation on system I.

The statistic numbers of the bound and unbound ions are shown in Table 1. In system I, almost all of the 20 Ca^{2+} ions (~ 18.7 of 20) bind to the POPG bilayer. About half of the 20 Mg^{2+} ions (~ 9.8 of 20) are bound ions. In contrast, only a small portion of Na^+ and K^+ ions are bound into the lipid bilayer, so that ~ 125.9 of the 160 Na^+ ions and ~ 135.3 of the 160 K^+ ions still stay in the bulk solvent. In system II, ~ 55.5 of 60 Ca^{2+} ions, ~ 4.9 of 40 Mg^{2+} ions, ~ 3.5 of 40 Na^+ ions, and ~ 4.2 of 80 K^+ ions are bound ions. It is thus suggested that different ion mixtures result in very different compositions of the bound ions and that Ca^{2+} is always the predominant bound ion among the four ions. To directly show the interaction probability of these ions to the membrane, we calculated the probability profile of each ion along the reaction coordinate ζ (Figure S3, Supporting Information). In agreement with the numbers of bound ions (Table 1), Ca^{2+} binds to the membrane with much higher probability than other ions.

Ion–Lipid Interactions. The interaction modes of different pure ions with lipid bilayers have been widely investigated by using MD simulations.^{14–18,35,36} However, to our knowledge, limited results have been reported for the interaction modes of an ion within an ion mixture with lipid bilayers. Consequently, a question arises of whether a pure ion and this ion in an ion mixture adopt a same binding mode with lipid bilayer or not. In order to answer this question, we analyzed the ion–lipid interactions in the two simulation systems by calculating two parameters, the number of each type of oxygen per bound with which the ion interacts and the number of lipid molecules per bound with which the ion interacts.

The cations bind to lipids by forming interactions with lipid oxygens through direct coordination bonds and/or water bridges. In system I, each Ca^{2+} , Mg^{2+} , Na^+ , and K^+ ion interacts with ~ 5.7 , ~ 3.9 , ~ 6.6 , and ~ 6.7 oxygens, respectively (Table 1). In system II, the corresponding oxygens interacting with these ions decrease to ~ 5.3 , ~ 3.1 , ~ 4.7 , and ~ 5.9 , respectively (Table 1). This result indicates that the four ions interact with less lipid oxygens in system II than in system I. Additionally, Ca^{2+} , Mg^{2+} , Na^+ , and K^+ ions have different modes to interact with the lipids (Figure 2). In general, Ca^{2+} ions mainly interact with the POPG lipids by coordination bonds, while water-bridge-mediated interaction dominates the binding between Mg^{2+} ions and the POPG lipids. For the Na^+ ion, coordinations and water-bridge-mediated interactions contribute almost equally to the binding with POPG lipids, and for the K^+ ion, water-bridge-mediated interactions contribute slightly more to the ion–lipid binding than coordination in system I, but these two types of interactions are almost equal in system II (Figure 2).

Oxygens $\text{O}_{\text{C}3}$, $\text{O}_{\text{C}2}$, O_{13} , O_{14} , O_{11} , O_{12} , O_{22} , and O_{32} of POPG lipid are involved in the interactions with ions (Figure 2). The Ca^{2+} ion shows the highest selectivity in binding with these oxygen atoms, and it is more inclined to bind to O_{13} and O_{14} through coordination bonds and prefer to interact with O_{22} through water bridges in both systems I and II (Figure 2). In

contrast, Mg^{2+} , Na^+ , and K^+ ions show different selectivities for the oxygens in the two systems. In system I, which contains only 20 Ca^{2+} ions, about ~ 60.6 lipids do not interact with Ca^{2+} ions, thereby providing more opportunities for Na^+ , K^+ , and Mg^{2+} ions to bind with the lipids. In this system, these three types of ions mostly form water bridges with O_{13} and O_{14} . In system II, where 40 more Ca^{2+} ions were added, almost all of the lipids (~ 126.5 out of 128 lipids) are bound with Ca^{2+} ions; thereby, the other three ions have less probability to bind to the oxygen atoms. These results suggest that the binding modes of Mg^{2+} , Na^+ , and K^+ ions are different in different ion mixtures and could be influenced by Ca^{2+} concentration.

Another parameter to describe the ion–lipid interactions is how many lipid molecules interact per ion. On average, a bound Ca^{2+} ion binds to nearly four POPG molecules in both systems, and other cations bind to less POPG molecules per ion (Figure 3). Moreover, Mg^{2+} , Na^+ , and K^+ ions interact with

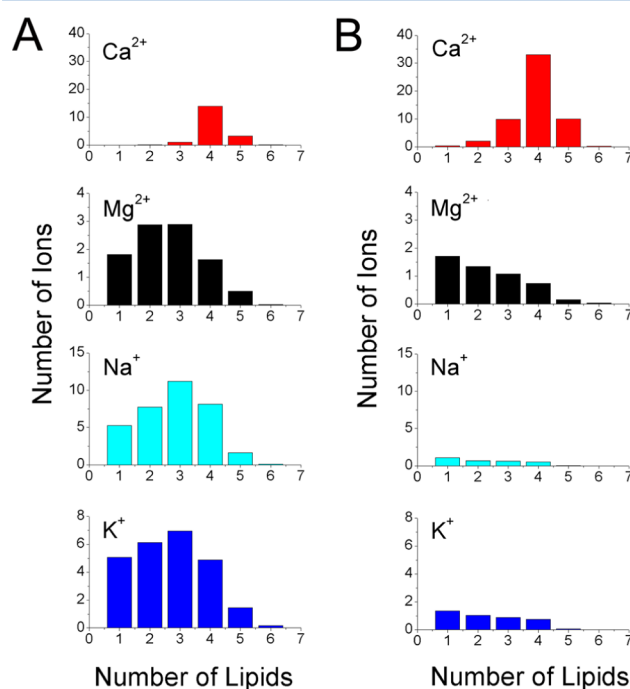


Figure 3. Average numbers of ions binding to one, two, three, four, five, or six lipids in systems I (A) and II (B).

different numbers of lipids in the two systems. In system I, with a lower concentration of Ca^{2+} ion, most of the bound Mg^{2+} , Na^+ , and K^+ ions interact with two or three lipids per ion. However, most of the bound Mg^{2+} , Na^+ , and K^+ ions only interact with one lipid in system II, in which many more Ca^{2+} ions exist than in system I. These results again suggest that different ion mixtures will affect the interaction modes of the ion–lipid complex and also show the regulative functionality of Ca^{2+} ions to the interaction modes of other ions to the lipids. Figure 4 shows the last snapshots of the two systems, presenting a vivid view of the ion–lipid interactions. In both systems, one bound Ca^{2+} ion interacts with four phosphoric acid groups of the surrounding POPG lipids, and a $\text{Ca}^{2+}(\text{POPG})_4$ complex is thus formed. When more Ca^{2+} ions are bound to lipids in system II, almost all of the phosphoric acid groups of the lipids are involved in binding with Ca^{2+} ions, and clusters composed of few POPG lipids are generated. Other ions only occupy the gap area between the clusters. This

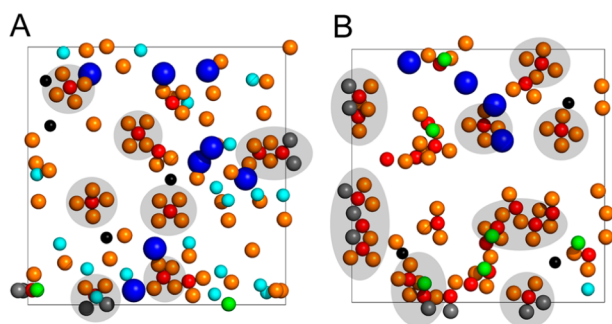


Figure 4. Structural views of the ion–lipid interactions in the last snapshots of systems I (A) and II (B). Black squares show the periodical box in the x – y plane (parallel to the membrane surface). Ca^{2+} , Mg^{2+} , Na^+ , K^+ , and Cl^- ions and phosphorus atoms are shown as red, black, cyan, blue, green, and orange balls, respectively, and the phosphorus atoms from the neighboring periodical box are shown as gray balls. Ca^{2+} ions that bind with four phospholipids are highlighted in gray circles.

demonstrates again that the binding of Mg^{2+} , Na^+ , and K^+ ions with POPG is strongly affected by the concentration of Ca^{2+} ions in the lipid bilayers.

Binding Affinities of the Ions to POPG Lipids. From the binding modes and competition states of Ca^{2+} , Mg^{2+} , Na^+ , and K^+ , we can qualitatively deduce the relative binding affinities of these ions with the POPG bilayer. In system I, the concentrations of Ca^{2+} and Mg^{2+} ions are the same, but the number of bound Ca^{2+} ions to the lipid bilayer is much larger than that of bound Mg^{2+} ions (Table 1). This indicates that during binding with POPG bilayer, the Ca^{2+} ion is stronger in competition with the Mg^{2+} ion. In system II, ~ 4.9 of 40 Mg^{2+} ions and ~ 3.5 of 40 Na^+ ions are bound ions (Table 1), suggesting that Mg^{2+} has a stronger lipid binding affinity than Na^+ . In addition, ~ 34.1 of the 160 Na^+ ions and ~ 24.7 of the 160 K^+ ions in system I are bound ions (Table 1), indicating that the binding affinity of Na^+ is higher than that of K^+ . Taken together, we can conclude that the binding affinities of the four ions with POPG lipids are in the following order, $\text{Ca}^{2+} > \text{Mg}^{2+} > \text{Na}^+ > \text{K}^+$, which is in agreement with previous experimental and simulation results.^{17,18,37–40}

In order to obtain quantitative data for the lipid binding of these ions, we calculated the binding free energies of these ions with a POPG lipid bilayer using the potentials of mean force (PMF) approach based on the MD simulations. The profile of PMF for each ion binding to the membrane can be calculated from the ion probability profile (Figure S3, Supporting Information) by using eq 1 (see the Methods section). The calculation results are shown in Figure 5. The PMF profile of each ion in either system I or system II has an energy well, from which we can calculate the binding free energy of the ion to the lipid bilayer. The calculated binding free energies of the four ions are listed in Table 2. The binding affinities of the four ions are in the order of $\text{Ca}^{2+} > \text{Mg}^{2+} > \text{Na}^+ > \text{K}^+$, as indicated by the calculated binding free energies of these four ions with lipids in both systems (Table 2). This quantitative result is in agreement with the above qualitative result (Table 1). The binding free energy calculation also demonstrates the dominance of the Ca^{2+} ion in competition with the other three ions, Mg^{2+} , Na^+ , and K^+ . In system I, Ca^{2+} ion binding with the POPG bilayer has a binding free energy of about -4.2 kcal/mol, and the binding free energies of Mg^{2+} , Na^+ , and K^+ ions are about 60, 36, and 24% of the Ca^{2+} ion. In system II, the binding free energy of the

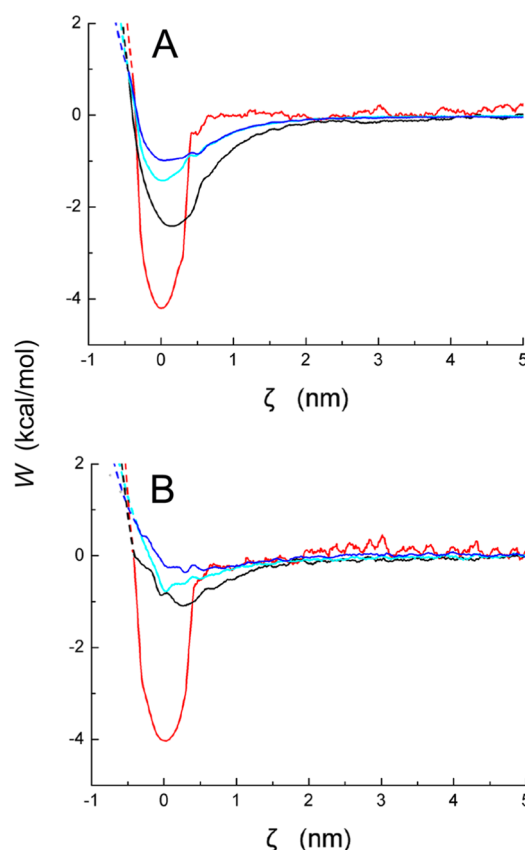


Figure 5. Potentials of mean force (PMF) for Ca^{2+} (red), Mg^{2+} (black), Na^+ (cyan), and K^+ (blue) ions along z coordinates in systems I (A) and II (B). For visualization, the curves were smoothed by an average of the adjacent five points.

Ca^{2+} ion is almost not changed in comparison with that in system I; however, the binding affinities of the other three ions remarkably decreased to about 50% of those in system I (Table 2). This result provides quantitative values for the conclusion that the binding of Mg^{2+} , Na^+ , and K^+ ions to the lipids is mediated by the concentration of the Ca^{2+} ion.

Kinetics of Ion Binding and Unbinding. To further rationalize the binding selectivity of the POPG lipid bilayer for ions, we estimated the kinetic parameters (t'_{on} , t_{off} , k'_{on} , and k_{off}) in addition to estimating the binding affinities for the four ions. The four kinds of kinetic parameters were calculated by using eqs 3, 4, 6, and 7, and the results are also listed in Table 2. The calculation results indicate that the binding rates (on-rates) of Ca^{2+} and Mg^{2+} are about 5–10 time faster than those of Na^+ and K^+ , while the unbinding rates (off-rates) of Ca^{2+} and Mg^{2+} are about 10–5000 time slower than those of Na^+ and K^+ . In particular, the residence time of the Ca^{2+} ion is much longer than that of the other three ions. These data indicate that Ca^{2+} ion has a characteristic of fast binding and slow unbinding compared with other ions, which is beneficial to the competition for the Ca^{2+} ion in binding to the POPG lipid bilayer. Comparing the data of systems I and II, we can notice that in these two systems, the kinetic parameters of the Ca^{2+} ion are kept the same; however, in system II, the binding rates of Mg^{2+} , Na^+ , and K^+ become slower, and their unbinding rates tend to be faster than those in system I. This result suggests in the viewpoint of kinetics that, in the ion mixture, increasing the concentration of Ca^{2+} ions may weaken the capability of other ions (Mg^{2+} , Na^+ , and K^+) to bind to the lipid bilayer.

Table 2. Thermodynamic and Kinetic Parameters of Ion–Lipid Binding

	system I				system II			
	Ca ²⁺	Mg ²⁺	Na ⁺	K ⁺	Ca ²⁺	Mg ²⁺	Na ⁺	K ⁺
ΔPMF (kcal/mol)	−4.2	−2.5	−1.5	−1.0	−4.1	−1.1	−0.9	−0.5
conc. (mM)	1.18	9.32	114.67	123.33	4.32	31.33	33.37	67.70
t'_{on} (ns)	19.5	2.08	3.46	2.62	11.3	5.14	7.26	6.27
t_{off} (ns)	280.5	2.00	0.94	0.48	144.9	0.71	0.70	0.35
k'_{on} ($10^9 \text{ mol}^{-1} \text{ s}^{-1}$)	43	52	2.5	3.1	21	6.2	4.1	2.4
k_{off} (10^9 s^{-1})	0.0036	0.50	1.1	2.1	0.0069	1.4	1.4	2.9

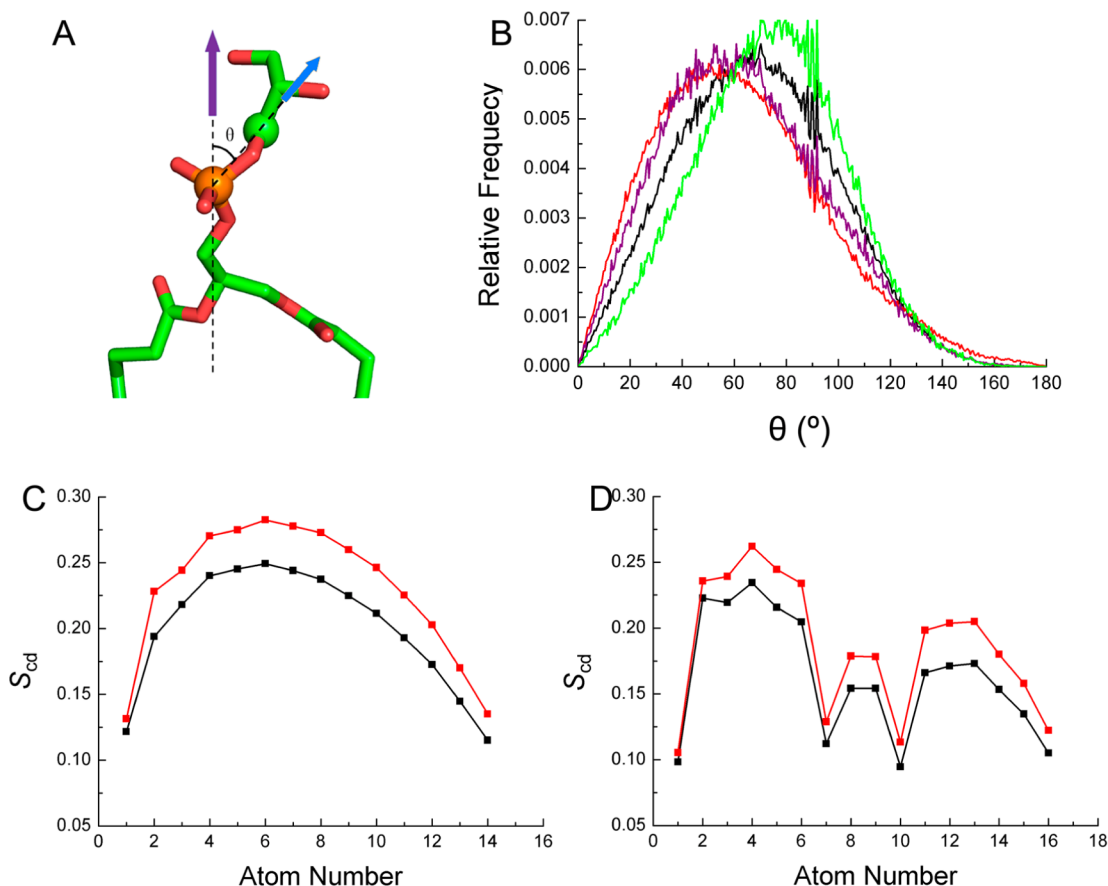


Figure 6. Lipid structures in systems I and II. (A) Orientation of the head group of POPG described by the angle (θ) between the P → C11 vector (blue arrow) and the outward bilayer normal (purple arrow). (B) θ angle distributions of all lipids in system I (black), Ca^{2+} bound to lipids in system I (purple), lipids that do not interact with Ca^{2+} ions (green), and all lipids in system II (red) are displayed. The averaged θ values of systems I and II are $\sim 71^\circ$ and $\sim 63^\circ$, respectively. In our previous MD simulations on single ions, the average θ values of systems with Ca^{2+} , Na^+ , and K^+ ions were $\sim 67.2^\circ$, $\sim 74.5^\circ$, and $\sim 94.5^\circ$ respectively.¹⁸ (C) The ordering parameter of sn-1 chains of POPG in systems I (black) and II (red). (D) The ordering parameter of sn-2 chains of POPG in systems I (black) and II (red).

Structures of the POPG Bilayer under Different Ion Mixture Conditions. The above analyses indicate that different ion mixtures result in different compositions of the bound ions and different ion–lipid interaction modes. In the following, the effects of the two ion mixtures on the structures of the POPG bilayer are analyzed on the basis of four calculated parameters, the area per lipid, bilayer thickness, head group orientation, and ordering of hydrophobic tails.

The area per lipid (A_L) and bilayer thickness ($D_{\text{p-p}}$) are two important geometrical parameters that represent the level of shrinking or swelling of the lipid bilayer.⁴¹ The bilayer thickness, involved in lipid–protein hydrophobic matching that regulates membrane protein function,⁴² can be monitored as the average distance between the two phosphorus atoms from two layers in the normal. The A_L values of POPG in

systems I and II are ~ 57.1 and $\sim 53.4 \text{ \AA}^2$, respectively, and the thicknesses of the bilayers of these two systems are respectively ~ 37.8 and $\sim 43.2 \text{ \AA}$ (Figure 1). This calculation data suggest that the bound ions in system II integrate lipids more efficiently than those in system I.

Due to electrostatic attraction, cations strongly interact with negative-charged head groups and thereby affect the head group orientation. Here, the head group orientation is defined by the angle between the P → C11 vector and the normal axis of bilayer (θ angle, Figure 6A).¹⁸ This angle reflects the PG head group orientation as follows: an angle of 0° or 90° implies that the PG head group is almost vertical or parallel to the membrane surface. Figure 6B plots the probability distributions of the θ angle of POPG lipids in the two systems. The angle probability distribution profiles of systems I and II (black and

red curves in Figure 6B, respectively) are quite different. The peaks of the profiles for systems I and II are ~ 70 and $\sim 50^\circ$, respectively. The averaged θ values of systems I and II are ~ 71 and $\sim 63^\circ$, respectively. These data demonstrate that the head groups of POPG lipids in system I are more parallel to the membrane surface than those in system II.

The ordering of hydrophobic tails is a typical structure parameter of the lipid. The mobility of membranes is associated with the ordering of lipid acyl chains.⁴³ The deuterium order parameter (S_{cd}) is usually used to describe the ordering of lipid acyl chains. The S_{cd} values of sn-1 and sn-2 chains for the two systems are plotted in Figure 6C and D, respectively. The plots of the two systems share similar patterns. However, the S_{cd} value of each carbon atom in system II is larger than that of the corresponding carbon atom in system I, especially the middle atoms in both chains, indicating a more ordered POPG tail in system II. The snapshots shown in Figure 1 also give a general view of the ordering of the lipid acyl chains in the two systems.

The above analysis on the area per lipid, bilayer thickness, head group orientation, and ordering of hydrophobic tails for systems I and II reveals that the lipid bilayer is arranged more tidily and tightly in the environment with a higher concentration of Ca^{2+} . This result is in agreement with the conclusion revealed by our previous study on pure ion–lipid bilayer interactions, which suggested that higher Ca^{2+} concentration causes a more tight and ordered arrangement of the lipid molecules.¹⁸

■ DISCUSSION

Binding Competition of the Ions to Lipids. Previous studies on comparisons of ion binding abilities were performed based on the simulations and measurements for the interactions of lipid bilayers with individual ion species rather than ions in ion mixtures,^{38,39,44–46} which could not reflect the competition of ions in binding with lipids. In the present study, we designed two systems for MD simulations to elucidate the competition capability for each ion species in binding with the lipids. System I contains an ion mixture of 20 Ca^{2+} , 20 Mg^{2+} , 160 Na^+ , and 160 K^+ ions, and system II includes 60 Ca^{2+} , 40 Mg^{2+} , 40 Na^+ , and 80 K^+ ions (Table 1). MD simulations on these two systems could not only differentiate the binding capability of the ions to the lipid but also address the influence of one ion (e.g., Ca^{2+}) to the binding of other ions to the lipid. From the numbers of bound ions to the lipid derived from the MD trajectory on system I, we may conclude that the binding capability of Ca^{2+} is stronger than that of Mg^{2+} , and the binding capability of Na^+ is stronger than that of K^+ , and the analysis of the bound ion numbers on MD simulations of system II may reveal that the binding affinity of Mg^{2+} is larger than that of Na^+ (Table 1). From the bound ion numbers revealed by MD simulations, we can conclude qualitatively that the binding capability of these ions to the lipid is in an order of $\text{Ca}^{2+} > \text{Mg}^{2+} > \text{Na}^+ > \text{K}^+$. Moreover, binding free energies of the four ions to the lipid bilayer were also estimated by using the PMF approach based on the MD simulations (Table 2), giving a same but more quantitative conclusion for the binding affinity of the four ions.

Newton et al. determined the intrinsic binding constants (K_i values) for Ca^{2+} , Mg^{2+} , and Na^+ ions to anionic PS vesicles, which are 35.0, 4.0, and 0.8 mol^{-1} , respectively.³⁹ These binding constants can be converted into binding free energies by the relation of $\Delta G^\circ = -RT \ln K_i$ (where T is the absolute temperature and R is the universal gas constant). The

conversion results in binding free energies for these three ions to the anionic PS vesicles are, respectively, -2.1 , -0.8 , and 0.1 kcal/mol. Another experiment determined K_i values of Ca^{2+} and Na^+ to monolayer and lamellar PS lipids to be 10^4 and 6.65 mol^{-1} ,³⁸ and the converted binding free energies were -5.5 and -1.1 kcal/mol, respectively. Our calculated binding free energies of Ca^{2+} , Mg^{2+} , and Na^+ to the POPG bilayer are in good agreement with the above-mentioned experimental data,^{37–40} indicating the reliability of our simulation and computational results (Table 2).

It is easy to understand that ions with two positive charges (Ca^{2+} and Mg^{2+}) bind to the membrane stronger than the ones with one positive charge (Na^+ and K^+). Intuitively, it is difficult to understand that the Ca^{2+} ion binds to the membrane more strongly than the Mg^{2+} ion does because the size of the latter is smaller than that of the former. Indeed, the radial distribution functions (RDFs) of the Mg^{2+} –O and Ca^{2+} –O distances derived from the MD simulations indicate that the former is shorter than the later (Figure S4A, Supporting Information), which is in agreement with the experimental data and quantum chemistry calculations.⁴⁷ On average, either the Mg^{2+} ion or Ca^{2+} ion may coordinate six oxygens, as indicated by the integrating profiles of the RDFs (Figure S4B, Supporting Information), which is also in agreement with the experimental and theoretical data.⁴⁸ This result also indicates that the Mg^{2+} ion seems to bind the membrane more tightly than the Ca^{2+} ion does. However, our MD results indicate that Ca^{2+} ions bind to the membrane mainly via direct coordination bonds with lipid oxygens, while Mg^{2+} ions mostly interact with the membrane through water bridges, that is, the ion coordinates with a water molecule, which further hydrogen bonds to a lipid oxygen (Figures 2 and S1, Supporting Information). This implies that the structure of POPG lipids is more suitable for Ca^{2+} binding than for Mg^{2+} binding. In addition, both experimental and computational results indicate that the hydration energy of the Mg^{2+} ion is larger than that of the Ca^{2+} ion.^{49,50} All of these facts facilitate the Ca^{2+} ion in binding to the membrane in comparison with the Mg^{2+} ion. According to this notion, the binding affinity of the K^+ ion to the membrane should be stronger than that of the Na^+ ion. Nevertheless, because the size of K^+ is too large (much larger than that of the Ca^{2+} ion) to fit into the cave composed of lipids (Figures S1, Supporting Information), the bound K^+ ions could distort the structures of the lipids. This is one of the reasons why the binding affinity of the Na^+ ion is larger than that of the K^+ ion, although these two ions bind to the membrane in a similar mode (Figure 2). Taken together, Ca^{2+} is an ion that may tightly bind to the membrane due to its proper size and balance ability for coordinating with lipid oxygens and water oxygens.

Employing a similar method to simulate ligand–receptor binding,^{33,34} we calculated the kinetic parameters (k'_{on} , k_{off} , t'_{on} , and t_{off}) for ions binding and unbinding with lipids (Table 2). The result suggests that the stronger competitive capability of Ca^{2+} in binding to the POPG bilayer is majorly determined by its small off-rate k_{off} (long residence time $t_{\text{off}} = 1/k_{\text{off}}$). The differences of the on-rates of these ions are not so obvious, whereas the k_{off} value of Ca^{2+} is 2–3 orders of magnitude smaller than that of other ions; thereby, the Ca^{2+} ion has to take a much longer time to leave the bilayer than the other ions do. Therefore, the kinetic data explain that the strongest binding affinity of Ca^{2+} to the lipids is mostly due to its smallest off-rate.

Influences of Ion Mixtures on the Structures of POPG Lipids. Studies on ion–lipid interactions based on the MD

trajectory of a certain ion species and lipids suggested that different ions show different ion–lipid interactions.^{16,18,51} Our work confirms this conclusion by observing that different ions show differential interactions with lipid oxygens. Ca^{2+} , Mg^{2+} , Na^+ , and K^+ ions bind to different numbers and/or types of lipid oxygens (Figures 2–4). Furthermore, we found that the same type of ions behave differently in binding with lipid oxygens in different concentrations. Compared to system I, Mg^{2+} , Na^+ , and K^+ ions in system II prefer to form more water bridges with hydroxyl group oxygens instead of with lipid oxygens. In particular, Mg^{2+} ions interact with lipids mainly through water bridges in system I, while Mg^{2+} ions interact with POPG through both coordination bonds and water bridges in system II. However, the Ca^{2+} –lipid oxygen interactions are almost conserved in both systems. These results indicate that the binding modes of Na^+ , K^+ , and Mg^{2+} ions with POPG are affected by the compositions of the ion mixture. However, the binding mode of the Ca^{2+} ion with the lipid is not affected by the change of the content of the ion mixture. Additionally, the binding affinity of Ca^{2+} to the lipids almost does not change from system I to system II, and that of other ions to the lipids change dramatically (Table 2). Owing to the dominating role of Ca^{2+} ions, the structure of the lipid bilayer in system II shows a remarkable difference from that in system I, indicating that the lipids arrange more orderly and tightly in system II. As a result, the structure of the POPG bilayer is most influenced by Ca^{2+} ions rather than other ions (Figures 4 and 6). In comparison with other ions, in particular, with Mg^{2+} , Ca^{2+} ions influence the POPG bilayer through stabilizing and tightening of the structure of the bilayer (Figure 6). This result implies that in biological systems, Ca^{2+} may regulate the functions of some membranes or membrane proteins by changing the concentration, as will be discussed below.

Biological Implications. In our previous study,¹⁸ we discussed the biological implication of Ca^{2+} effects on anionic lipids and the regulation mechanisms of Ca^{2+} ions through affecting the membrane structures. Obviously, the present study continuously supports the hypothesis proposed in the previous study. A very important conclusion of our MD simulations is that Ca^{2+} ions may quickly and concentration-dependently regulate (mostly tighten and order) the structures of anionic lipid bilayer, and Ca^{2+} ions dominate the effects in regulating the bilayer structure if there are other ions around the membrane (Figure 6). This implies that Ca^{2+} ions should also play important roles in tightening and ordering the structures of lipid rafts. The alteration of the bilayer structure might cause a hydrophobic mismatching of the proteins. To seek better hydrophobic matching to the surrounding lipids, these proteins may change their conformation to minimize this mismatching, which would further bring in the changes of their functions.⁵² The alternation of the head group orientation may also influence the protein–lipid interaction because it would result in different patterns of hydrogen bonds between lipid head groups and the membrane proteins. The hydrogen bonds between lipid oxygens and proteins are important for the membrane proteins to anchor at the lipid–water interface.⁵² Therefore, the changes of both the head group orientation and the hydrophobic thickness of the bilayer due to Ca^{2+} –lipid interaction may exert appreciable effects on membrane proteins. The spatial and temporal distribution of calcium ions usually fluctuates in a very large scale, that is, in cytosol, usually 10–100 nM at rest and up to 200–300 μM locally for signaling transduction after stimulation.^{53,54} Given that Ca^{2+}

shows significant effects on the lipid bilayer and embedded proteins, the changes of Ca^{2+} concentration should play important roles in regulating a broad range of biological processes.

The present study also indicates the different roles of Ca^{2+} and Mg^{2+} in membrane fusion. Membrane fusion is a ubiquitous reaction involved in many cellular processes.⁵⁵ It has been revealed that anionic lipids, such as PG and PS, are critical to membrane fusion, and the interactions between divalent cations and anionic lipids are distributed to the membrane fusion.⁸ Divalent cations Ca^{2+} and Mg^{2+} play essential roles in membrane fusion for their high binding affinities to anionic lipids. However, both the rate and extent for Mg^{2+} to induce fusion are much lower than those of Ca^{2+} .⁵⁶ In our simulations, it has been shown that Mg^{2+} has a much lower binding affinity in both systems for anionic POPG lipids than Ca^{2+} (~ 1.7 kcal/mol lower in system I and ~ 3.0 kcal/mol lower in system II). Moreover, the binding modes between Mg^{2+} and Ca^{2+} to POPG are different. Mg^{2+} is hard to dehydrate and thereby binds lipids dominantly through water bridges, which may be due to its higher dehydration energy.⁵¹ The stable hydration is a disadvantage for Mg^{2+} to bind to anionic lipids without water molecules and make the newly formed membrane interface leaky while inducing fusion.⁵⁶ In contrast, Ca^{2+} is easier to dehydrate and can coordinate directly to the lipid oxygens (Figures 2 and S1, Supporting Information). It can be supposed that during the Ca^{2+} -induced fusion, the negatively charged head groups of lipids from the two membrane bilayers may aggregate for the coordination bonds between the lipid oxygens and Ca^{2+} ions. In sum, the different mechanisms of membrane fusion induced by Ca^{2+} and Mg^{2+} may be attributed to their different binding abilities and modes to anionic lipids.

CONCLUSION

To investigate the effects of ion mixtures on membrane structures, we have carried out long-time MD simulations (3.6 μs in total) on two large POPG bilayers with different ion mixtures composed of Ca^{2+} , Mg^{2+} , Na^+ , and K^+ ions. The simulations gain new insights into the ion mixture effects on membranes and also provide a good explanation for a variety of biological processes relevant to Ca^{2+} and Mg^{2+} .

We have elucidated the energetics and kinetics for the binding of these ions to the POPG bilayer. It has been revealed that the binding efficiency of the cations with POPG lipids is in the order of $\text{Ca}^{2+} > \text{Mg}^{2+} > \text{Na}^+ > \text{K}^+$. The binding free energy of Ca^{2+} to the lipid bilayer is ~ -4.0 kcal/mol, which is much lower than those of other ions. The on-rates of different ions do not have a large difference, while the off-rate of Ca^{2+} is 2–3 orders of magnitude smaller than those of the others. Therefore, the strongest binding affinity of Ca^{2+} is mainly determined by its smallest off-rate.

Our work also cast new insights into the binding modes between ions and lipids. We found that the same type of ions behave differently in binding with lipid oxygens in different concentrations. Furthermore, we have observed the phenomenon that the binding modes of certain ions could be influenced by other ions. In our simulations, the binding modes of Mg^{2+} , Na^+ , and K^+ to the lipids are influenced by the concentration of Ca^{2+} . In addition, our study suggests that the structure of the lipid bilayer is influenced dominantly by the concentration of Ca^{2+} ions.

■ ASSOCIATED CONTENT

■ Supporting Information

Typical modes of the ion–lipid binding (Figure S1), numbers of the bound ions as a function of simulation time (Figure S2), probabilities of ion appearance along ζ coordinates (Figure S3), and RDF analysis of oxygens around Ca^{2+} (red) and Mg^{2+} (Figure S4). This material is available free of charge via the Internet at <http://pubs.acs.org>.

■ AUTHOR INFORMATION

Corresponding Author

*E-mail: hljiang@mail.shcnc.ac.cn. Tel: +86-21-50805873. Fax: +86-21-50807088 (H.J.); E-mail: hy_yang@mail.shcnc.ac.cn. Tel: +86-21-50800619. Fax: +86-21-50807088 (H.Y.).

Notes

The authors declare no competing financial interest.

■ ACKNOWLEDGMENTS

This work was supported by National Natural Science Foundation of China (31100594 and 21021063), the State Key Program of Basic Research of China (2009CB918502), and Shanghai Science and Technology Development Funds (11ZR1444400 and 12QA1404000). Computational resources were supported by the National Supercomputing Center in Tianjin, the Shanghai Supercomputer Center, and the Computer Network Information Center of the Chinese Academy of Sciences.

■ REFERENCES

- (1) Parsegian, V. A. *Ann. N.Y. Acad. Sci.* **1975**, *264*, 161–171.
- (2) Watts, A.; Harlos, K.; Marsh, D. *Biochim. Biophys. Acta* **1981**, *645*, 91–96.
- (3) Hauser, H.; Shipley, G. G. *Biochemistry* **1984**, *23*, 34–41.
- (4) Loosley-Millman, M. E.; Rand, R. P.; Parsegian, V. A. *Biophys. J.* **1982**, *40*, 221–232.
- (5) Akutsu, H.; Seelig, J. *Biochemistry* **1981**, *20*, 7366–7373.
- (6) Clarke, R. J.; Lupfert, C. *Biophys. J.* **1999**, *76*, 2614–2624.
- (7) Berridge, M. J.; Bootman, M. D.; Roderick, H. L. *Nat. Rev. Mol. Cell Biol.* **2003**, *4*, 517–529.
- (8) Papahadjopoulos, D.; Nir, S.; Duzgunes, N. *J. Bioenerg. Biomembr.* **1990**, *22*, 157–179.
- (9) Deamer, D. W. *J. Bioenerg. Biomembr.* **1987**, *19*, 457–479.
- (10) Lande, M. B.; Donovan, J. M.; Zeidel, M. L. *J. Gen. Physiol.* **1995**, *106*, 67–84.
- (11) Gerke, V.; Creutz, C. E.; Moss, S. E. *Nat. Rev. Mol. Cell Biol.* **2005**, *6*, 449–461.
- (12) Arbuzova, A.; Murray, D.; McLaughlin, S. *Biochim. Biophys. Acta, Rev. Biomembr.* **1998**, *1376*, 369–379.
- (13) Stephen, R.; Filipek, S.; Palczewski, K.; Sousa, M. C. *Photochem. Photobiol.* **2008**, *84*, 903–910.
- (14) Bockmann, R. A.; Grubmüller, H. *Angew. Chem., Int. Ed.* **2004**, *43*, 1021–1024.
- (15) Pedersen, U. R.; Leidy, C.; Westh, P.; Peters, G. H. *Biochim. Biophys. Acta* **2006**, *1758*, 573–582.
- (16) Cordomi, A.; Edholm, O.; Perez, J. J. *J. Phys. Chem. B* **2008**, *112*, 1397–1408.
- (17) Vernier, P. T.; Ziegler, M. J.; Dimova, R. *Langmuir* **2009**, *25*, 1020–1027.
- (18) Yang, H.; Xu, Y.; Gao, Z.; Mao, Y.; Du, Y.; Jiang, H. *J. Phys. Chem. B* **2010**, *114*, 16978–16988.
- (19) Vermeer, L. S.; de Groot, B. L.; Reat, V.; Milon, A.; Czaplicki, J. *Eur. Biophys. J.* **2007**, *36*, 919–931.
- (20) Pedersen, U. R.; Peters, G. H.; Schroder, T. B.; Dyre, J. C. *J. Phys. Chem. B* **2010**, *114*, 2124–2130.
- (21) Humphrey, W.; Dalke, A.; Schulten, K. *J. Mol. Graphics* **1996**, *14*, 33–38.
- (22) Jorgensen, W. L.; Chandrasekhar, J.; Madura, J. D.; Impey, R. W.; Klein, M. L. *J. Chem. Phys.* **1983**, *79*, 926–935.
- (23) Hess, B.; Kutzner, C.; van der Spoel, D.; Lindahl, E. *J. Chem. Theory Comput.* **2008**, *4*, 435–447.
- (24) Lindahl, E.; Bjelkmar, P.; Larsson, P.; Cuendet, M. A.; Hess, B. *J. Chem. Theory Comput.* **2010**, *6*, 459–466.
- (25) Feller, S. E.; MacKerell, A. D. *J. Phys. Chem. B* **2000**, *104*, 7510–7515.
- (26) MacKerell, A. D.; Klauda, J. B.; Venable, R. M.; Freites, J. A.; O'Connor, J. W.; Tobias, D. J.; Mondragon-Ramirez, C.; Vorobyov, I.; Pastor, R. W. *J. Phys. Chem. B* **2010**, *114*, 7830–7843.
- (27) Bussi, G.; Donadio, D.; Parrinello, M. *J. Chem. Phys.* **2007**, *126*, 014101.
- (28) Berendsen, H. J. C.; Postma, J. P. M.; Vangunsteren, W. F.; Dinola, A.; Haak, J. R. *J. Chem. Phys.* **1984**, *81*, 3684–3690.
- (29) Miyamoto, S.; Kollman, P. A. *J. Comput. Chem.* **1992**, *13*, 952–962.
- (30) Hess, B.; Bekker, H.; Berendsen, H. J. C.; Fraaije, J. G. E. M. *J. Comput. Chem.* **1997**, *18*, 1463–1472.
- (31) Essmann, U.; Perera, L.; Berkowitz, M. L.; Darden, T. A.; Lee, H.; Pedersen, L. G. *J. Chem. Phys.* **1995**, *103*, 8577–8593.
- (32) Roux, B. *Comput. Phys. Commun.* **1995**, *91*, 275–282.
- (33) Buch, I.; Giorgino, T.; De Fabritiis, G. *Proc. Natl. Acad. Sci. U.S.A.* **2011**, *108*, 10184–10189.
- (34) Shan, Y. B.; Kim, E. T.; Eastwood, M. P.; Dror, R. O.; Seeliger, M. A.; Shaw, D. E. *J. Am. Chem. Soc.* **2011**, *133*, 9181–9183.
- (35) Elmore, D. E. *FEBS Lett.* **2006**, *580*, 144–148.
- (36) Broemstrup, T.; Reuter, N. *Biophys. J.* **2010**, *99*, 825–833.
- (37) McLaughlin, S.; Mulrine, N.; Gresalfi, T.; Vaio, G.; McLaughlin, A. *J. Gen. Physiol.* **1981**, *77*, 445–473.
- (38) Hauser, H.; Darke, A.; Phillips, M. C. *Eur. J. Biochem.* **1976**, *62*, 335–344.
- (39) Newton, C.; Pangborn, W.; Nir, S.; Papahadjopoulos, D. *Biochim. Biophys. Acta* **1978**, *506*, 281–287.
- (40) Eisenberg, M.; Gresalfi, T.; Riccio, T.; McLaughlin, S. *Biochemistry* **1979**, *18*, 5213–5223.
- (41) Ipsen, J. H.; Mouritsen, O. G.; Bloom, M. *Biophys. J.* **1990**, *57*, 405–412.
- (42) Mouritsen, O. G.; Bloom, M. *Annu. Rev. Biophys. Biomol. Struct.* **1993**, *22*, 145–171.
- (43) Seelig, J. *Q. Rev. Biophys.* **1977**, *10*, 353–418.
- (44) McLaughlin, S. G.; Szabo, G.; Eisenman, G. *J. Gen. Physiol.* **1971**, *58*, 667–687.
- (45) Hauser, H.; Phillips, M. C.; Levine, B. A.; Williams, R. J. P. *Eur. J. Biochem.* **1975**, *58*, 133–144.
- (46) Tatulian, S. A. *Eur. J. Biochem.* **1987**, *170*, 413–420.
- (47) Pavlov, M.; Siegbahn, P. E. M.; Sandström, M. *J. Phys. Chem. A* **1998**, *102*, 219–228.
- (48) Katz, A. K.; Glusker, J. P.; Beebe, S. A.; Bock, C. W. *J. Am. Chem. Soc.* **1996**, *118*, 5752–5763.
- (49) Marcus, Y. *J. Chem. Soc., Faraday Trans.* **1991**, *87*, 2995–2999.
- (50) Hummer, G.; Pratt, L. R.; García, A. E. *J. Phys. Chem.* **1996**, *100*, 1206–1215.
- (51) Jiao, D.; King, C.; Grossfield, A.; Darden, T. A.; Ren, P. *J. Phys. Chem. B* **2006**, *110*, 18553–18559.
- (52) Lee, A. G. *Biochim. Biophys. Acta* **2004**, *1666*, 62–87.
- (53) Bootman, M. D.; Collins, T. J.; Peppiatt, C. M.; Prothero, L. S.; MacKenzie, L.; De Smet, P.; Travers, M.; Tovey, S. C.; Seo, J. T.; Berridge, M. J.; Ciccolini, F.; Lipp, P. *Semin. Cell Dev. Biol.* **2001**, *12*, 3–10.
- (54) Bootman, M. D.; Berridge, M. J. *Cell* **1995**, *83*, 675–678.
- (55) Jahn, R.; Lang, T.; Sudhof, T. C. *Cell* **2003**, *112*, 519–533.
- (56) Wilschut, J.; Duzgunes, N.; Papahadjopoulos, D. *Biochemistry* **1981**, *20*, 3126–3133.